ISSN 2278-2540 | DOI: 10.51583/IJLTEMAS | Volume XV, Issue VIII, August 2026

Covalent Immobilization of Invertase on Methacrylic Acid-Based Nanogel & its Specialty Application in Biomedical Field

***Lok Raj Sharma**

HOD Department of Chemistry, LBS Govt. Degree College Saraswatinagar Sawra, Shimla 171206, India

DOI: https://doi.org/10.51583/IJLTEMAS.2026.150800121

Received: 02 September 2026; Accepted: 08 September 2026; Published: 21 September 2026

ABSTRACT

Nano-bioreactors are becoming increasingly important in the chemical transformations. The nano-size of the enzyme support provides large surface area for the covalent binding between its functional sites and those of the biocatalyst. In the present study, invertase extracted from Saccharomyces cerevisiae was immobilized on the functional copolymeric nanogels by the covalent binding via azide method. The immobilized enzymes were tested for sucrose hydrolysis activity by standard DNS method spectrophotometrically at λ_{max} = 540 nm. The immobilized-invertase was tested for stability after 30 days of its storage and reused for 12 continuous cycles. Covalent binding results in improving the spectrum of enzyme activity over a larger range of temperature and pH as high activity was observed even at 65 °C and a wide range of pH, hence, covalent immobilization on the nanogels stabilized invertase over a wide range of operating conditions than its free form. The nanogels with and without the immobilized invertase was characterized by the nitrogen analysis, FTIR, SEM, XRD, TEM and elemental analysis (% nitrogen estimation) which provide the evidence of covalent binding of invertase on the functional surface of the nanoparticles. The kinetics of the sucrose hydrolysis by the invertase-immobilized nanogels was determined by the Lineweaver-Burke plot or Eddie-Hofstee model. The value of V_{max} (0.249 unit/mg), K_m (14.89 mol/L) and E_a (2.697 kj/mol) were calculated for the immobilized invertase, and these are significantly different than those obtained for the free invertase.

INTRODUCTION

Stimuli-responsive polymeric gels are attractive options for the design of the smart materials for various applications, and these can be used to bio-mimick a specific molecule[1]. The stimuli-responsive properties of hydrogels are of special interest to develop and design materials as the drug delivery vehicles, biosensors, separation materials, soft actuators, and for use in many biological applications[2–11]. The use of hydrogels for the immobilization of enzymes on the Hydrogel materials is currently a very active area of research to generate smart materials those apart from offering uses as the heterogeneous catalysts are more stable to their external environment than the free form of the enzymes. These advantages of the immobilized-enzyme over its free form are dependent on the nature of the enzyme and support used, and the mode of immobilization. A good match of these factors may result in the conformational changes that enzyme undergoes after immobilization that results in the enhanced activity and improved stability for use at the wide range of the operating conditions. On the contrary, improper selection of the support and mode of immobilization may result in the loss of activity due to steric and diffusional restrictions caused by the immobilization[12]. The immobilization process often results in the enhanced stabilization under storage as well as operational conditions with respect to denaturation by high temperature, pH and organic solvents or autolysis, and often broadens the applicable pH range[13]. It is desirable that the easy recovery, operational stability, prolonged storage and high reusability are ensured while designing the support and mode of immobilization to realise the development of a continuous bioprocesses.

ISSN 2278-2540 | DOI: 10.51583/IJLTEMAS | Volume XV, Issue VIII, August 2026

Out of different modes of immobilization[14-16], the covalent immobilization is the best mode[17], as the other modes of immobilization like entrapment of the enzyme within a matrix restricts the entry of the substrate to the enzyme active sites or the physical adsorption by weak interactions results in an easy leaching out of the enzyme on the reuse. The covalent linkages, however, may consume the active sites of the enzyme and results in the decreased activity[18]. The use of hydrogels as immobilization support provides a natural environment for the enzyme. The covalent immobilization of enzymes on the pre-functionalized supports is relatively easy. Functional nanogels are promising candidates for use as support in the enzyme immobilization as these have large surface area due to its nano scale size, ease of anchoring of functional groups for enzyme attachment, hydrophilic character to help enzyme retain their tertiary structure, and toxicological safety. The hydrophilic character, high surface area, high porosity, mechanical and chemical stability, and surface chemical activity are some primary considerations in the selection of support used in the enzyme immobilization[19].

Owing to these attributes of hydrogels the polyacrylamide-based hydrogels are widely reported for the immobilization of different enzymes[20]. Invertase has been immobilized covalently on various carriers such as porous glass[21,22], activated clay[23], corn stover[24,25], bead cellulose, glycidyl methacrylate[26], styrene-divinyl benzene copolymer[26,27], nanoparticles of granular chicken bone[28] or magnetic silica[29], but the immobilization of invertase by chemical coupling on the functionalized polymeric nanogels is not described. In our previous work we reported some natural or synthetic polymers as supports for the enzyme immobilization[30-33], but none of these was of nano-scale.

In view of the above, we report synthesis of an active nanogel that has all the above listed desirable characteristics as the support of the invertase extracted from Saccharomyces cerevisiae. Methacrylic acid, which exhibits both thermo and pH sensitivity, along with acrylamide, which is a good adsorbent, was used to synthesize crosslinked copolymeric nanogels, which were further functionalized to the azide form on which invertase was immobilized though a covalent linkage. The as-prepared nanogels and its immobilized form were characterized with FTIR, SEM, XRD, TEM and elemental analysis provide the evidence of the synthesis and structure-property relationship.

Experimental Section

Material used

Acrylamide (AAm), ammonium per sulphate (APS), buffer tablets [S.D. Fine Chem. Ltd., Mumbai, India], methacrylic acid (MAAc), ethylene glycoldimethylacrylate (EGDMA) [Merck, Schuchardt, Germany] yeast invertase concentrate [BDH company], were used as received.

Synthesis of nanogels

An equimolar mixture of methacrylic acid (MAAc) and Acrylamide (AAm) was taken with ethyleneglycol dimethylacrylate (EDGMA) [1% of the total weight of the two monomers] and ammonium persulphate (0.5% of the combined weight of two monomers), respectively, as crosslinker and initiator were all taken together in a minimum quantity of water (1mg/ml just to solubilize different reaction components). All these were transferred to the chemical reactor (M/s. Autochem, US) and stirred for 5 min and thereafter polymerization was allowed to proceed at 70 °C for 30 min. The hydrogel of poly(MAAc-co-AAm)-cl-EGDMA was obtained as monolith which was stirred with distilled water to remove any soluble fractions present. It was dried for 48 h at 40 ºC in the air oven. There after it was cut to disks of definite length and diameter, washed again and dried in hot air vacuum oven at 40 °C to obtain a constant weight.

The hydrogel was grounded to fine powder was dispersed in an equimolar mixture of dodecanol and water at 33°C±2°C was stirred with exposure to the sunlight on an electro-magnetic heater cum-stirrer for total 48 h. The gelation in the reaction mixture decreased the gel particle size to the nano-scale. Nanogels were separated by precipitation by using distilled acetone as non-solvent, again washed with acetone and water continuously till the dodecanol was fully removed. Nanogels were dried in the vacuum oven at 25 °C until the original weight was observed.

ISSN 2278-2540 | DOI: 10.51583/IJLTEMAS | Volume XV, Issue VIII, August 2026

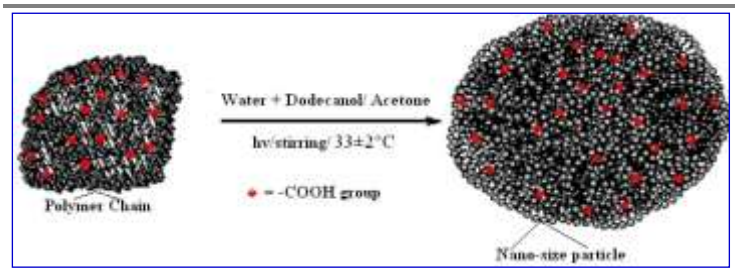

2.3. Functionalization of nanogels

The nanogel was converted into azide by the Curtius azide by following an earlier reported procedure.[34, 35]

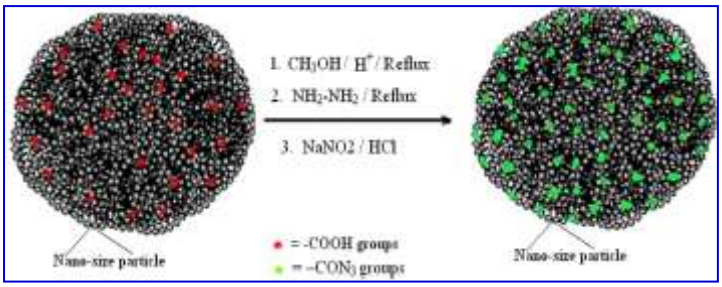

Immobilization of invertase on nanogel

The carboxyl groups of the nanogels were converted to the azide groups. Functionalized polymers containing azide groups were used for the enzyme immobilization by coupling reactions via the amino groups of invertase to form a covalent linkage[36, 37]. Hydrogels or their nano-forms were taken separately in a known quantity and mixed with an equal volume of 0.1 M phosphate buffer (pH 5.0) and enzyme solution (1.4 mL of water, 0.5 mL of phosphate buffer and 0.1 mL of 20 times diluted invertase in each set of test tube). It was shaken in a shaker at 4 °C for 1 h and later stirred in an ice bath till the maximum %immobilization was obtained. Enzyme contents were estimated by the spectrophotometric method (Miller, 1959) using Folin–reagent and absorption measured at 640 nm in a UV–Vis spectrophotometer by using enzyme as blank in buffer at pH 4.5. The invertase-immobilized nanogel was washed three times with 20 mL of 100 mM acetate buffer (pH 4.5) and stirred between each wash. Three successive washings were found to be enough to remove the physically adsorbed invertase. The thoroughly washed gels were taken and stored at 7 °C until used. The solution after each wash tested for the invertase with standard DNS method. The thoroughly washed gels were taken and stored at 7 °C until used. %covalent immobilization (%C_I) was calculated by subtracting the total amount of invertase left after immobilization in the solution (R_p) and collected from each wash from (W_p) the total protein contents taken and expressed in % as shown below.

$$\%C_I = T_p-(R_p + W_p)/T_p \times 100$$

%covalent immobilization efficiency was calculated from the activity measurement of the free and the immobilized enzyme at the standard conditions of temperature and pH as follows:

$$\eta = A_I/A_f$$

$$\%I = \eta \times 100$$

Where η is the efficiency of support for covalent immobilization and A_I and A_f are the activities of the immobilized and free invertase, respectively.

Characterization of nanogels

The as-prepared, the azide form and the invertase-immobilized form, were characterized by nitrogen analysis (Carlo Erba Instrument 1150 analyzer or Elementar Vario El) scanning electron micrography (Joel

ISSN 2278-2540 | DOI: 10.51583/IJLTEMAS | Volume XV, Issue VIII, August 2026

Stereoscan-150 microscope), Fourier transform infrared spectroscopy (Nicollet 5700), X-ray diffraction study (SIMENS D5005 X-ray Diffractrometer) and transmission electron microscopic (TEM) images of nanogels were obtained on A-JEOL 1200 EXII transmission electron microscope operating at an accelerating voltage of 80 kV with the direct magnification ranging from 60,000-4,00000.

Invertase activity and assay

Invertase hydrolyzes the non-reducing β-d-fructofuranoside residues of sucrose to yield invert sugar. The invert sugar on reaction with 3, 5-dinitrosalicylic acid (DNS) produces the colour change which is proportional to the amount of the invert sugar released, which in turn is proportional to the invertase activity of the sample. The absorbance was measured at λ_{max} 540 nm and converted into micromoles of the reducing sugar produced using a standard curve. One invertase unit is the amount of invertase which will produce 1 micromole of reducing sugar (expressed as invert sugar) per minute under the conditions specified in this procedure. Invertase activity assay was performed in a batch reactor by taking 0.1 g immobilized invertase which was mixed with 1.4 mL, 0.1 M phosphate buffer (pH = 6.0), 10% sucrose solution (1.0 mL) and shaken in a water bath-cum-shaker at 45 °C. In the case of free invertase, instead of 0.1 g immobilized enzyme, 0.1 mL invertase (diluted 20 times) was used. After the required time (70 min), it was mixed with 5 mL of DNS reagent and heated in a boiling water bath for 5 min. and cooled to room temperature and the amount of the reducing sugar was measured spectrophotometrically at 540 nm. The concentration of the invert sugar produced was calculated from the invert sugar standard curve and specific activity of the free and the immobilized invertase was calculated using the following method:

Specific activity (unit/minute/g) = $[(C_S-C_B) \times \text{dilution}]/W$

Where C_S and C_B are contents of invert sugar in the experimental and blank solution and

W is the weight of sample in g. %Relative activity (%R) of the immobilized invertase was

calculated from following equation:

$\%R = (S_i / S_f) \times 100$

Where, S_i and S_f are the specific activity (unit/min/g) of immobilized and free invertase,

RESULTS AND DISCUSSION

Synthesis and characterization of nanogels supports

The three dimensional cylindrical hydrogel networks were synthesized following a green approach and the final yield of 99.7% was obtained with respect to the total amount of the monomer taken**.** These hydrogel networks were further converted into nanogels with 98% yield and carboxylic acid moiety of the nanogels was further functionalized to azide through Curtius-azide method. The evidence of the synthesis of the as-prepared nanogel and their consequent functionalization to the azide and the invertase-immobilized forms were obtained by characterization by the nitrogen analysis, FTIR, SEM, XRD and TEM. The increase in %nitrogen, from the as-prepared nanogel (6.448%) to its azide form (12.54%) revealed the presence of $–N_3$ group by modification of the carboxylic groups, by 51.41 times provides evidence of functionalization.

The comparison of the FTIR spectra of the three different forms is presented in (figures 1a, 1b and 1c). These provide the evidence of the functionalization as strong absorption peaks near 1300 cm^{-1} due to the $-N_3$ symmetric stretching. In comparison, the appearance of the –C=O starching between 1750-1700 cm^{-1} is evidence of the $-N_3$ linked –C=O group of acid and amide which appear at 1701.1 cm^{-1} and 1654.6 cm^{-1} in its precursor. Intense peak at 3467.5 cm^{-1} and 3425.7 cm^{-1} in the precursor indicate the -OH and –NH stretching, respectively. In the invertase-immobilized sample, the appearance of a peak at 3100-3070 cm^{-1} due to the $–NH_3^+$ stretching of the amino acid of invertase and 1580-1485 cm^{-1} is due to symmetric bending

ISSN 2278-2540 | DOI: 10.51583/IJLTEMAS | Volume XV, Issue VIII, August 2026

of $–NH_3^+$ of amino acid of invertase is present. The intense peak appears at 1290 cm^{-1}, due to the in-plane bending of $–NH_3^+$ group of amino acid. \

SEM images reveal the effect of functionalization and invertase immobilization on the particle morphology as the change in the surface structure after each step. SEM images before functionalization (figures $2A_1$ and $2A_2$), after functionalization to azide form (figures $2B_1$ and $2B_2$) and invertase immobilization (figures $2C_1$ and $2C_2$) reveal the appearance of rough surface after the azide formation and a smooth surface for the invertase-immobilized nanogels. These two observations result from the mechanical effect in the former and the interaction of the surface functionality to form covalent cluster structures throughout the surface of the nanoparticles in the latter. TEM images of the as-prepared, functionalized and the invertase-immobilized nanogels (figures 3A, 3B, $3C_1$ and $3C_2$). All images exhibits the particle size <100 nm and particle having semi-rod like structure. The images of the invertase-immobilized particles have the layer of the covalently-linked invertase on the surface of nanogels, which is better exhibited in the micrograph of higher magnification.

XRD patterns of the functionalized and immobilized nanogels are presented in (figures 4_A and 4_B). In the case of the functionalized nanogels, there is a peak at 2h = 26.5740 corresponding to a d-spacing of 3.35440 nm. This peak represents the plane analogous to the inter-layer spacing. After the invertase immobilization this peak shifted slightly to 2h=26.5558 with a d-spacing of 3.35388 nm demonstrating an expansion of layers thereby indicating that the activation takes place within the hydrogel surface. The intensity of the new peak is very high which shows that most of the nanogel layers are covalently interacting with the invertase. Immobilization with invertase does not change the intensity of the peak. There is a slight shifting of peak to lower values with very low intensity. This suggests that the enzyme interacts strongly with the surface group of nanogels. As the enzyme loading increased, the intensity of the new peak also increased confirming the interaction of enzyme into the nanogel layers. Covalent binding of invertase results in the enzyme intercalation. The d -spacing increased in the significant range. Complete shifting of the peak to lower values suggests that the covalent linkage of invertase has taken place. Enzymes being polymers of very large molecular size the possibility of the attachment of the whole enzyme within the inter-lamellar space can be ruled out. The particle size of gels calculated by using scherrer's formula presented as follows:

$$D_p = \frac{0.94\lambda}{\beta_{1/2}\cos\theta}$$

Where, Where λ is the wave length of X-ray in A°, d is path length and θ is peak position in degree and $\beta_{1/2}$ is peak position (FWHM) in degree and 0.94 is the shape factor k. Size was found out to be 42.33 and 93.24 nm, which is a strong evidence of the nanogel formation.

Activity study of the immobilized invertase

Invertase specific activity (unit/min/g) was determined using sucrose as substrate in acetate buffer, pH 4.5, and at 50 °C. The reaction was stopped by the addition of dinitrosalicylic acid (DNS) and the reducing sugars were quantified according to the Miller method by spectrophotometric analysis at λ_{max}= 540 nm. One unit of the enzymatic activity was defined as the amount of enzyme that released 1 mM of glucose per min under the assay conditions. The parametric study of the immobilized invertase was studied to obtained a set of the optimum conditions as a function of temperature (in the range from 25 °C to 75 °C), pH (from 2.0 to 12.0) using Tris–HCl (7.0–9.0) buffer and time or the substrate concentration, and the activity and reusability/stability of the immobilized invertase was compared with that of the free invertase.

The Specific activity of free (freshly diluted invertase) and the immobilized invertase (after 30 days of its storage) with the time variation is presented in (figure 5A). Free enzyme exhibited the maximum activity (218.14 unit/min/g Er±1.219**)** after 15-35 min, while the immobilized invertase attained the same (187.62 unit/min/g Er±0.993), with %I= 86.008 (% covalent immobilization efficiency) after 50 min which

ISSN 2278-2540 | DOI: 10.51583/IJLTEMAS | Volume XV, Issue VIII, August 2026

corresponds to the % relative activity of 93.51% which is very significant despite the covalent immobilization. It also confirms the storage stability of the immobilized invertase. Dilution factor (20 times diluted in present case) in the concentrated invertase also play key role in the activity determination of invertase with time.

Thermal deactivation of biocatalyst is one of the major causes for the activity decay, thus the evaluation of thermal stability of the biocatalyst is a key issue for the effective characterization of a bioconversion system. The free enzyme rapidly lost activity above 45 °C, which is typical of most enzymes in the Free State. Whereas a marked enhancement of the thermal stability was achieved with covalent immobilization, since a little activity loss was observed after 60 min at 60 °C (figure 5B). The activity of the immobilized invertase even at 60 °C was very high [188.84 unit/min/g (Er±1.313)] in comparison to that of the free enzyme [233.46 unit/min/g (Er±1.019) and with %I = 80.8875]. The % relative activity of the immobilized invertase found 545.32 at 65 °C and 238.83 at 25 °C. The high thermal stability of the immobilized invertase is resultant of the covalent immobilization and consequent conformational changes in the immobilized invertase. The result observed in present study of immobilized invertase stability with temperature is better than the reported in literature[39]. So the functional nanogels are better support for the same.

The effect of the variation of the pH of the reaction system on the activity of free or immobilized invertase is presented in (figure 5C). The immobilized-invertase showed very high stability at a wide range of pH from 17.34 unit/min/g (Er±0.914)) at pH 2.0 to 148.32 unit/min/g) at pH 12.0, with the highest activity plateau 183.88 unit/min/g (Er±1.109) between pH 5-7 that corresponds to the % relative activity of 79.05, the immobilized enzyme showed a little loss of activity after pH 10.5. On the other hand, the free invertase was observed to be effective only between pH ranges of 4.5-7.0 as the activity sharply decreased in the alkaline pH. Further it is important to observe that the presence and type of the matrix/support used in this study did not alter the optimum pH value, but the spectrum range shifted toward the alkaline side which is probably due to the H-ion repulsion of medium with the positively charged matrix create the microenvironment for the invertase binding[40], and the result is that the immobilized-invertase exhibited the better results in the alkaline medium [41, 42]. The variation of the substrate concentration and the amount of the immobilized-invertase was also studied at the optimum temperature and pH (figures 5D and 5F). The immobilized-invertase showed constant increase with an increase in the initial substrate concentration from (0.1- 0.6 mg/0.1mg of immobilized-invertase). After that it attained an equilibrium or showed a slight decrease due to the interference of an excess substrate concentration approaching the catalyst active sites, but the free enzyme attained the maximum activity and catalysed the maximum substrate (0.1- 0.9 mg/0.1ml of the free diluted invertase) due to the better access to the active sites in this case.

Reusability cycle of immobilized invertase

The feasibility and the application of an immobilized-enzyme system in a large-scale process mainly depend on its operational stability. In order to evaluate this key parameter in the present system, the repeated batch runs were performed at 50 °C in pH 5.0 and 1 M substrate concentration (figure 5F). The activity of the same sample of the immobilized-invertase was studied by reusing it time and again till 12 cycles. A decrease in the activity was observed after 8 cycles (50.55 unit/min/g, Er±1.003), which may be due to the loss of the linked invertase from the surface which resulted in a low activity of 3.99 unit/min/g in the 10^{th} cycle of the successive use.

Determination of K_m, V_{max} and E_a

The kinetic values (K_m, V_{max}) for the immobilized-invertase were calculated from the standard Michelis-Menten (figures 6A and 6C) and Lineweaver-Burk plot (figures 6B and 6D). The values of K_m and V_{max} were calculated from the plot computationally and the data obtained for both free and immobilized-invertase was then plotted in the Michelis-Menten, Lineweaver-Burk and Eadie-Hofstee plots. The kinetic parameters, K_m, V_{max} and E_a of the free and immobilized enzymes were determined at constant temperature, pH while varying substrate concentrations. For invertase, enzyme activity profile was found to follow the Michaelis–Menten kinetics[43]. Therefore, K_m and V_{max} were obtained from the Lineweaver–Burk plots[44]. The lower K_m

ISSN 2278-2540 | DOI: 10.51583/IJLTEMAS | Volume XV, Issue VIII, August 2026

value of the immobilized invertase suggests an increased affinity of invertase to the substrate. In the present case it also showed better affinity for the nanogel which was not adversely affected by the covalent immobilization contrary to the reported significantly lower affinity of the immobilized invertase (higher K_m)[45].

In the present study, the substrate affinity of the invertase is also not affected by the covalent immobilization on the nanogel support as did not involve or caused hindrance to the active sites of the invertase. The variation in the V_{max} values after immobilization is also in agreement with the literature studies[46]. The dramatic decrease in V_{max} of the enzyme substrate reaction for the immobilized enzymes is caused by the hindrance to the approach of the substrate to the active sites of owing to the factors such as the structure of the support and efficiency of immobilization.

Eadie-Hofstee plot [V/[S] vs V] provided somewhat deviation from the linear behaviour plotted in (figures 6E and 6F). The non-linear distribution of points in this plot corresponds to the internal enzyme-substrate fluctuation during catalysis[47]. V_{max}/K_m and V_{max} and from the liner-fit corresponds with great accuracy to respective experimental value (Figures 6F). The V_{max} (248.1661) and V_{max}/K_m (177.7) from the Michelis-Menten equation were found comparable to those obtained Eadie-Hofstee plot V_{max} (246.36) and V_{max}/K_m (~160.00). Energy of activation (E_a) for the present bio catalytic reaction was determined by the use of Arrhenius-equation with the use of constant log K and log A calculated from Michelis-Menten equation at optimum condition of temperature (50 °C) and pH (4.5).

This is an important parameter for an immobilized-enzyme system as it indicates diffusion limitations[48]. It is postulated that the activation energy of the free invertase (4.856 kj/mol) is higher than that of the immobilized-invertase (2.697kj/mol) due to the influence of the intra-particle diffusion of substrate with the increasing particle size of gels in the solution phase. This indicates that the functional nanogel matrix reaction systems do not have the limitations of the internal diffusion but are more stable at higher temperatures due to the covalent bond formation[49].

It is concluded from these two kinetic parameters (V_{max} and K_m) that the involvement of the total diffusional resistance of the substrate to the active site leads to a loss of substrate affinity. Diffusional resistances were greater for the adsorbed invertase and less for the covalently bound invertase, despite the fact that, during covalent binding, the enzyme was intercalated in the nanogel matrix and caused pore blockage. This may be because the adsorption took place in the close proximity to the active site of invertase and therefore access to these sites was diminished further.

CONCLUSION

A new co-polymeric nanogel was synthesized and characterized by various techniques. It was used as a support for the covalent immobilization of invertase extracted from Saccharomyces cerevisiae. The nano-size of the support enhanced the affinity of support to the enzyme and despite covalent immobilization high activity if the immobilized invertase at wider operating conditions was observed. Apart from the high activity, storage stability, and reusability upto 8 cycles, the immobilized-invertase exhibited very high activity even at 65 °C and up to 12 pH, which are very high than its free form. The kinetics of the sucrose hydrolysis by the invertase-immobilized nanogels were determined by the Lineweaver-Burke plot or Eddie-Hofstee model also revealed that the covalently linked invertase has high affinity for the substrate as reflected from its V_{max}, K_m and E_a than that obtained for the free invertase. Thus, from the present work, it is revealed that the use of nanogels as support for the covalent immobilization of invertase is a productive process.

Acknowledgement

LRS acknowledges the University Grant Commission, New Delhi, India for providing necessary financial assistance for the same.

ISSN 2278-2540 | DOI: 10.51583/IJLTEMAS | Volume XV, Issue VIII, August 2026

REFERENCES

1. Matsumoto, A.; Ikeda, S.; Harada, A.; and Kataoka, K. Biomacromolecules **2003**, 4, 1410.
2. Hirokawa, Y.; Tanaka T. J. Chem. Phys. **1984**, 81, 6379.
3. Zhang, Y.; Tanaka, T. ; Shibayama, M. Nature **1992**, 360, 142.
4. Yoshida, R.; Uchida, K.; Kaneko, Y.; Sakai, K.; Kikuchi, A.; Sakurai, Y.; Okano, T. Nature. **1995**, 374, 240.
5. Bromberg, L. E.; Ron E. S. Adv. Drug Delivery Rev. **1998**, 31, 197.
6. Okajima, T.; Harada, I.; Nishio, K.; Hirotsu, S. J. Chem. Phys. **2002**, 116, 9068.
7. Schild, H. G. Prog. Polym. Sci. **1992**, 17, 163.
8. Okano, T. Adv. Polym. Sci. **1993**, 110, 180.
9. Sayil, C.; Okay, O. Polymer. **2001**, 42, 7637.
10. Hoffman, A. S.; Afrassiabi, A.; Dong L. C. J. Control. Rel. **1986**, 4, 213.
11. Bae, Y. H.; Okano, T.; Hsu, R.; Kim, S.W. Macromol. Chem. Rapid Commun. **1987**, 8, 481.
12. Trevan, M. D. Immobilized Enzymes: An Introd. and Appl. in Biotech. John Wiley & Sons Ltd. **1980**.
13. Schmid, A.; Dordick, J. S.; Hauer, B.; Kiener, A.; Wubbolts, M.; Witholt, B. Nature **2001**, 409, 258.
14. Hartmann, M.; Chem. Mater. **2005**, 17, 4577.
15. Sheldon, R. A. Adv. Synth. Catal. **2007**, 349, 1289.
16. Novick, S. J.; Dordick J. S. Biomaterials. **2002**, 23, 441.
17. Sharma, S.; Kaur, P.; Jain, A.; Moganty, R. R.; Gupta M. N. Biomacromolecules, **2003**, 4, 330.
18. Gill, I.; Ballesteros, A. J. Am. Chem. Soc. **1998**, 120, 8587.
19. Cabral, J. M. S.; Kennedy, J. F.; Taylor R. F. ed. Marcel Dekker, New York **1991**, pp. 73-138.
20. Wang, D.; Li, M.; He, B. Biotechnol. Appl. Biochem. **1992**, 16, 115-124.
21. Oshima, H.; Sakimoto, M.; Harano Y. Biotechnol. Bioeng. **1980**, 22, 2155-2167.
22. Mason, R. D.; Weetall, H. H. Biotechnol. Bioeng. **1972**, 14, 637-645.
23. Lopez, S. J.; Sola, C.; Lema, J. M. Biotechnol. Bioeng. **1982**, 24, 2721-2724.
24. Monsan, P.; Combes D. Biotechnol. Bioeng. **1984**, 26, 347-351.
25. Monsan, P.; Combes, D.; Alemzadeh, I. Biotechnol. Bioeng. **1984**, 26, 658-664.
26. Marek, M.; Valentova, O.; Kas, J. Biotechnol. Bioeng. **1984**, 26, 1223-1226.
27. Mansfeld, J.; Schellenberger A. Biotechnol. Bioeng. **1987**, 29, 72-78.
28. Findlay, C. J.; Pakin, K. L.; Yada, R. Y. Biotechnol. Left. **1986**, 8, 649-652.
29. Goetz, V.; Remaud, M.; Graves, D. J. Biotechnol. Bioeng. **1991**, 37, 614-626.
30. Pahujani, S.; Kanwar, S. S.; Chauhan, G. S.; Gupta, R. Bioresource Technology. **2008**, 99, 2566–2570.
31. Chauhan, G. S.; Kanwar, S. S.; Kaushal, R. K.; Kumar, Y.; Chauhan, S. J. Appl. Poly. Sci. **2008,** 108, 3200-3209.
32. Kanwar, S. S.; Chauhan, G. S.; Chimni, S. S.; Kumar Y.; Rawat, G. S.; Kaushal R. K. J. Appl. Poly. Sci. **2006**, 100, 1420-1426.
33. Kanwar, S. S.; Verma, H. K.; Kaushal, R. K.; Gupta, R.; Kumar, Y.; Chimni, S. S.; Chauhan, G. S. J. Appl. Poly. Sci. **2006**, 100, 4252–4259.
34. Silman, I. H.; Katchalski, E. Annu. Rev. Biochem. **1966**, 35, 873.
35. Maneche, G. Naturwissenschaften. **1964**, 51, 25.
36. Michael, F.; Ewers, J. Makromol. Chem. **1949**, 3, 200.
37. Mitz, M. A.; Summaria, L. J. Nature. **1961**,189, 576.
38. Lowry, O. H.; Rosebrough, N. J.; Faar, A. L.; Randall R. J. J. Biol. Chem. **1951**, 193,265.
39. Alkan, S.; Toppare, L.; Yagci, Y.; Yesim H. J. Biomater. Sci. Poly. Edn. **1999**, 10(12),1223-1235.
40. Tanriseven, A.; Dogan, S. Process Biochem. **2001**, 36, 1081.
41. Jafri, F.; Saleemuddin, M. Biotechnol. Bioeng. **1997**, 56, 605.
42. Sakakibara, M.; Wang, D.; Takahashi, R.; Takahashi, K.; Mori, S. Enz. Microb. Technol., **1996**, 18, 444.
43. Michaelis, L.; Menten, M. L. Biochem. **1913**, Z-49, 333.
44. Lineweaver, H.; Burk, D. J. Am. Chem. Soc. **1934**, 56, 658.

ISSN 2278-2540 | DOI: 10.51583/IJLTEMAS | Volume XV, Issue VIII, August 2026

45. Selampinar, F.; Akbulut, U.; Hoozden, M. Y.; Toppare, L. Biomaterials **1997**, 18, 1163.
46. Glick, N.; Landman, A. D.; Roufogalis, B. D. Trends in Biochem. Sci. **1979**, 4, N-82-N-83.
47. Bahar, T.; Tuncel, A. J. Appl. Polym. Sci. **2002**, 83(6), 1268–1279.
48. Miyamoto, K.; Fujii, T.; Tamaoki, N.; Okazaki, M.; Miura, Y. J. Ferment. Technol. **1973,** 51, 566–574.
49. Amaya-Delgado, L.; Hidalgo-Lara, M. E.; Montes-Horcasitas, M. C. J. Food Chem. **2006**, 99, 299–304.

Caption of Tables

Table 1. Represents the elemental analysis of poly[MAAc-co-AAm]-cl-EGDMA hydrogel after preparation, after functionalization and % yield of nanogel obtained.

Table 2. Represents the particle size evaluation from XRD analysis and % Covalent Immobilization of invertase obtained.

Table 3. Represents some kinetic parameter obtained for Immobilized and free invertase.

Table 4. Represents energy of activation for free and immobilized invertase.

Caption of Figures

Figure 1. FTIR spectra of poly[MAAc-co-AAm]-cl-EGDMA (A_0:-nanogel), (A: - Functionalized nanogel) (B:- invertase loaded nanogel).

Figure 2. SEM of poly[MAAc-co-AAm]-cl-EGDMA nanogel, functionalized nanogel and invertase loaded nanogel).

Figure 3. TEM of poly[MAAc-co-AAm]-cl-EGDMA (A:- nanogel) (B:- functionalized) nanogel (C and D:- invertase loaded nanogel).

Figure 4. XRD of poly[MAAc-co-AAm]-cl-EGDMA (A:- functionalized nanogel) (B:- Invertase loaded nanogel).

Figure 5. Specific and % relative activity study of free and poly[MAAc-co-AAm]-cl-EGDMA Immobilized invertase with time, Temperature, pH**,** substrate concentration, Enzymes concentration and Reusability plot.

Figure 6. Kinetic plot of free and poly[MAAc-co-AAm]-cl-EGDMA Immobilized invertase Michelis-Menten plot, Lineweaver-Burk plot and Eadie-Hofstee plot of free and immobilized invertase.

Figure 7. Arrhenius plot of free and poly[MAAc-co-AAm]-cl-EGDMA Immobilized invertase.

TABLE 1 Elemental Analysis of Hydrogels After Synthesis

	Samples after synthesis			**Samples After treatment with EDA**			
Samples	**% Nitrogen Found**	**% Carbon Found**	**% Hydrogen Found**	**% Nitrogen Found**	**% Carbon Found**	**% Hydrogen Found**	**%Yield Found After Synthesis**
Poly [MAAc-co-AAm]-cl-EGDMA	6.448	48.53	7.7	7.145	51.55	7.162	99.56

Nitrogen Analysis of Samples Before and After Functionalization					
Samples	% Nitrogen Before Functionalization	**% Nitrogen After Functionalization**	**% -COOH Experimental**	**% -COOH Theoretical**	**% -COOH Conversion into –CON3**
Poly [MAAc-co- AAm]-	6.448	12.54	51.4194	52.2891	98.31

ISSN 2278-2540 | DOI: 10.51583/IJLTEMAS | Volume XV, Issue VIII, August 2026

cl-EGDMA					
Some Useful Parameters Used in Preparation of Nanogel From Respective Hydrogel					
Samples	Initial Weight of Hydrogel Taken (g)	**Dodecanol /Water (1:1) Ratio (mL)**	**Total Time Taken Reaction for Completion (h)**	**Final weight Obtained After Conversion into Nanogel (g)**	**% Yield of Nanogels**
Poly [MAAc-co- AAm]-cl-EGDMA	2	100	64	1.988	99.4

TABLE 2

Some Useful XRD Parameters and Particle Size Analysis of Nanogels

Samples	**Position (°2θ)**	**FWHM(°2θ)**	**d-Spacing (A°)**	**Peak Area (ctc° 2θ)**	**Peak Intensity (%)**	**Particle Size (nm) at Fixed λ value**
Poly [MAAc-co-AAm]-cl-EGDMA	26.7004	0.8639	3.33881	225.48	100	9.8782

Invertase Immobilization Parameters and % Covalent Immobilization

Hydrogel Network	Tp × 102 (mg/mL)	Rp × 103 (mg/mL)	Wp × 103 (mg/mL)	Cp= Tp-(Rp+Wp)/Tp	%Cp= Tp-(Rp+Wp)/Tp×100
Poly(MAAc-co-AAm)-cl-EGDMA-G3	250	459	105	0.7744	77.44
Poly(MAAc-co-AAm)-cl-EGDMA-G2	250	631	139	0.692	69.2
Poly(MAAc-co-AAm)-cl-EGDMA-G1	250	616	496	0.5552	55.52

TABLE 3

Samples	**A×10-1**	**B×10-2**	**Sd**	**Vmax×103 (Unit/mg)**	**Km×10-2 (mol/L)**
Free Invertase	-0.314055	0.59999	1.38555	318.42	0.19102
Poly(MAAc-co-AAm)-cl-EGDMA-G3	-0.402972	0.59999	1.8475	248.16	0.14887
Poly(MAAc-co-AAm)-cl-EGDMA-G2	-0.777981	0.6	2.33976	128.53	0.07712
Poly(MAAc-co-AAm)-cl-EGDMA-G1	-0.175972	0.59999	1.26345	568.27	0.34134

Free Invertase				**Immobilized Invertase**			
Absorbance at λmax=540 nm	**Concentration (Cs-Cb)**	**1/[S]**	**1/V**	**Abs. at λmax=540 nm**	**Concentration (Cs-Cb)**	**1/[S]**	**1/V**
0.6209	0.7643	1.30839	78.50321	0.4201	0.3987	2.50815	150.489
0.7576	0.9853	1.01492	60.89516	0.4576	0.4502	2.22124	133.274
0.8501	1.1775	0.84926	50.95541	0.5931	0.6673	1.49858	89.914

ISSN 2278-2540 | DOI: 10.51583/IJLTEMAS | Volume XV, Issue VIII, August 2026

0.8497	1.1609	0.8614	51.68404	0.6764	0.8014	1.24782	74.868
0.85	1.1321	0.88331	52.99885	0.75	0.9232	1.08319	64.991
0.8498	1.1094	0.90139	54.08329	0.7501	0.9235	1.08284	64.97
0.8411	1.0784	0.9273	55.63798	0.7411	0.8884	1.12562	67.537
0.84	1.0784	0.9273	55.63798	0.74	0.8845	1.13058	67.834
0.8501	1.1155	0.89646	53.78754	0.7401	0.885	1.12994	67.796
0.7986	1.0184	0.98193	58.91595	0.6982	0.8284	1.20715	72.428

TABLE 4

Ea For Free and Immobilized Invertase/GOD on Functional Nanogel

Samples	**A**	**B**	**Ea (kj/mol)**
Free Invertase	0.63576	0.54458	4.52763
Poly(MAAc-co-AAm)-cl-EGDMA-Nanogel	0.93608	0.39678	3.29882
Poly(MAAc-co-AAm)-cl-EGDMA Azide	0.80414	0.47525	3 .95122
Poly(MAAc-co-AAm)-cl-EGDMA Precursor	0.91682	0.55368	4.60329

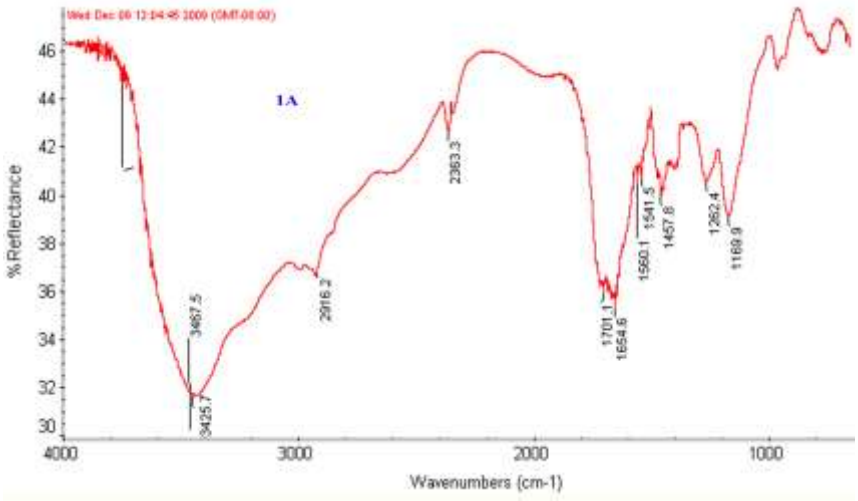

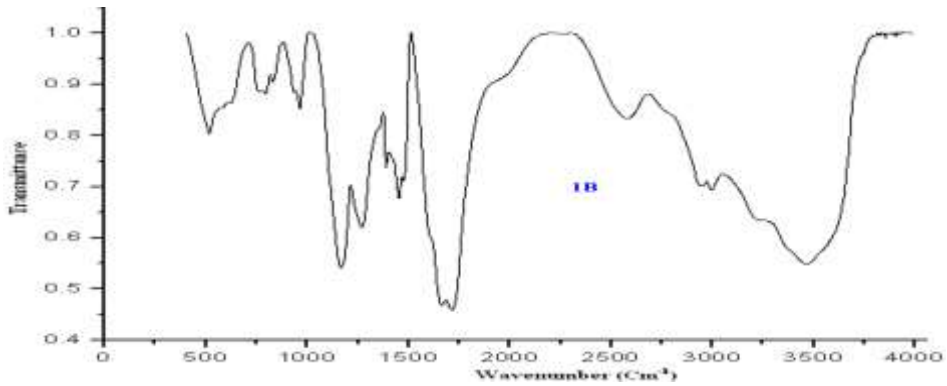

ISSN 2278-2540 | DOI: 10.51583/IJLTEMAS | Volume XV, Issue VIII, August 2026

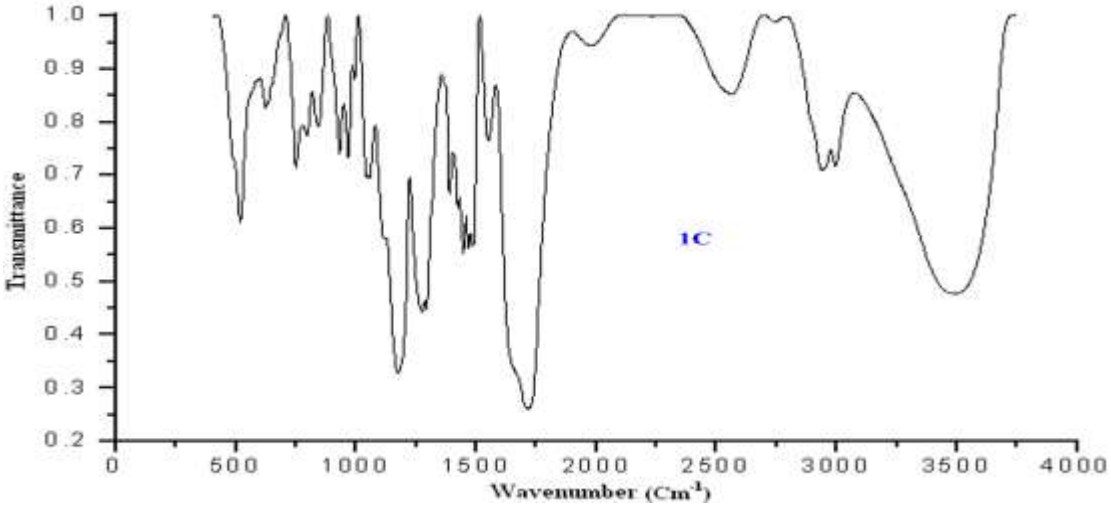

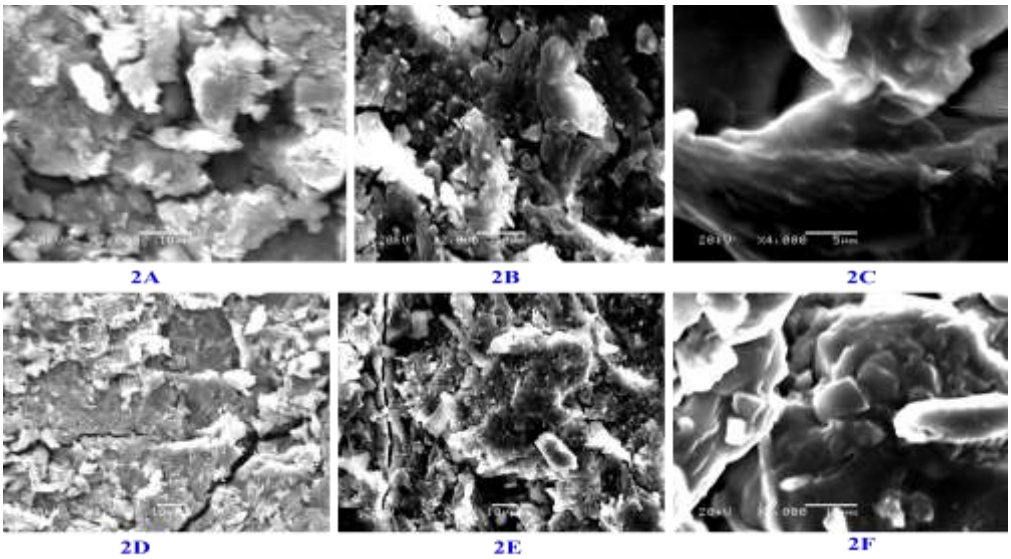

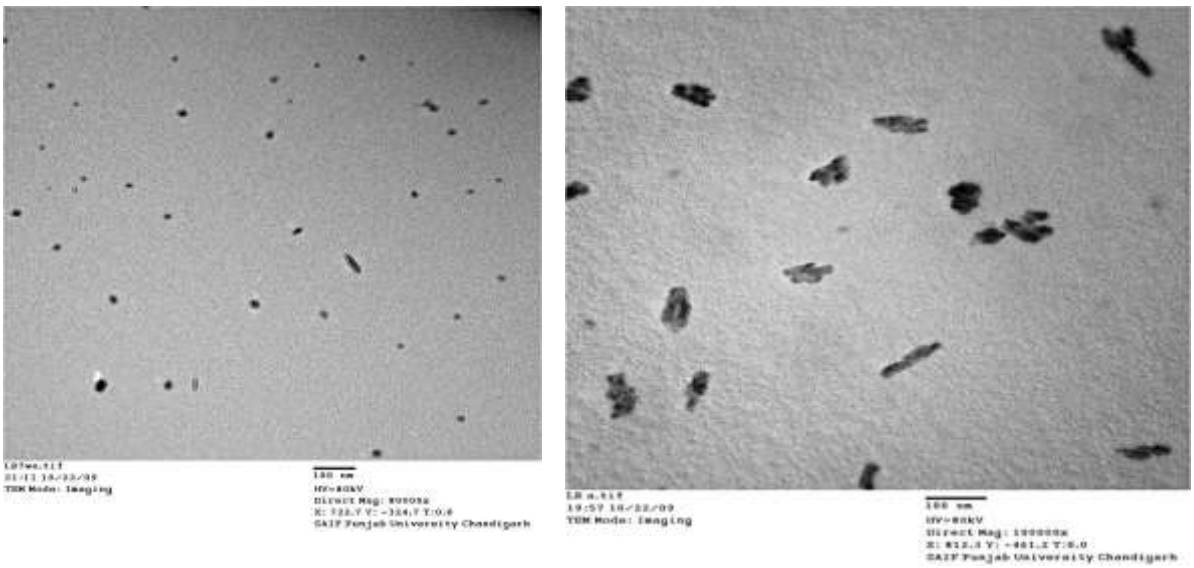

3A 3B

ISSN 2278-2540 | DOI: 10.51583/IJLTEMAS | Volume XV, Issue VIII, August 2026

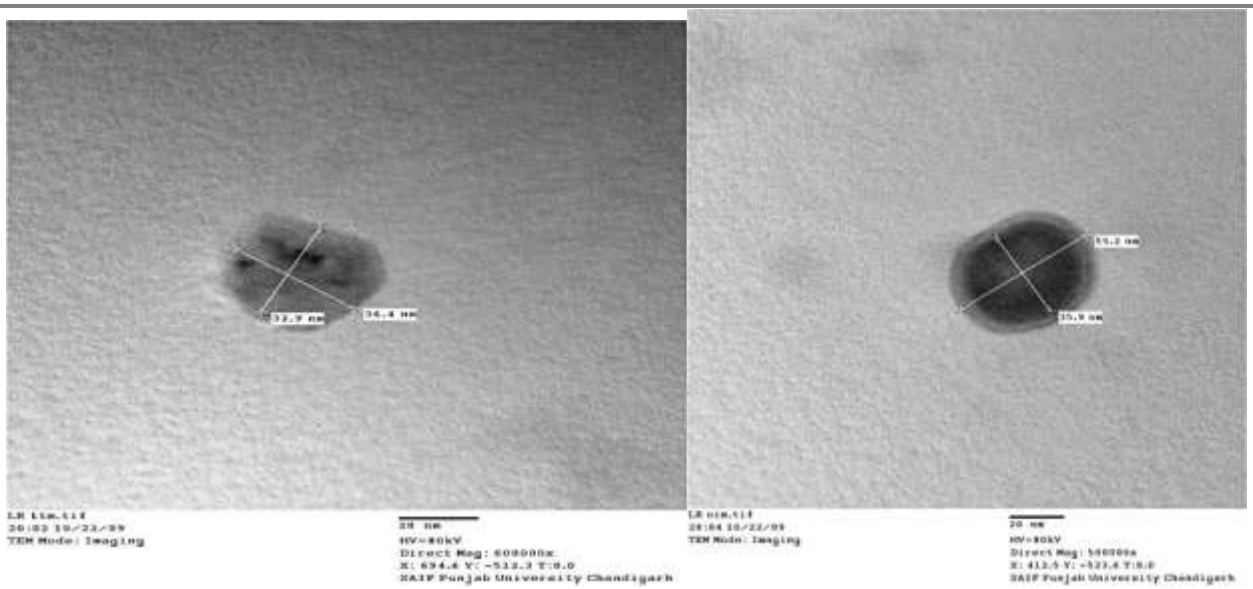

3C 3D

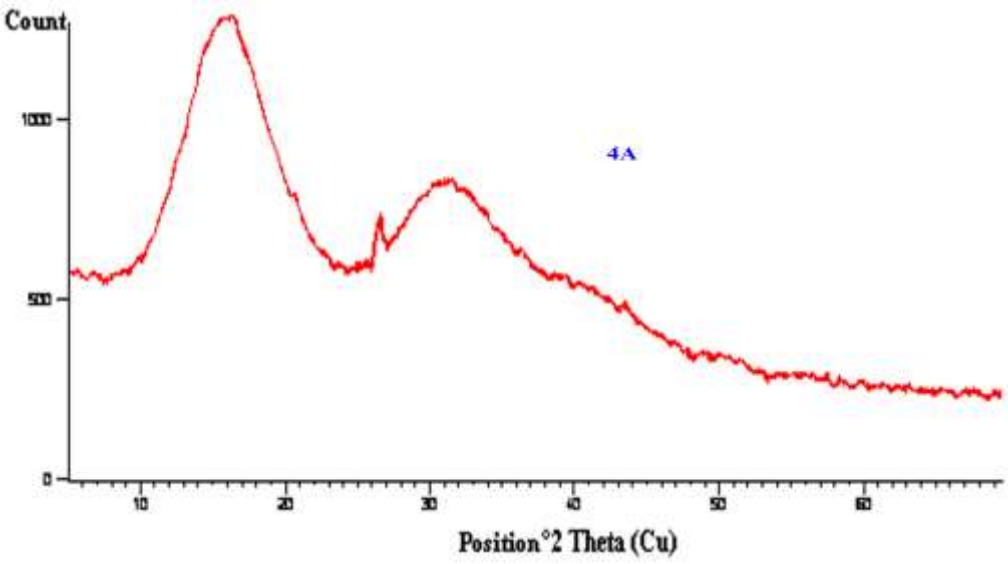

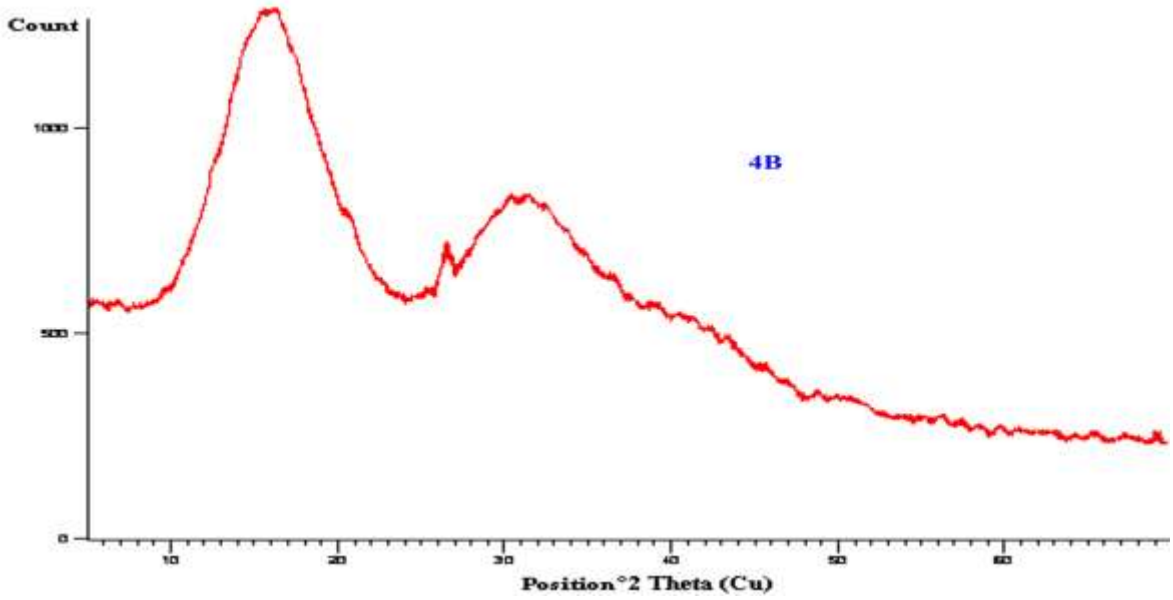

ISSN 2278-2540 | DOI: 10.51583/IJLTEMAS | Volume XV, Issue VIII, August 2026

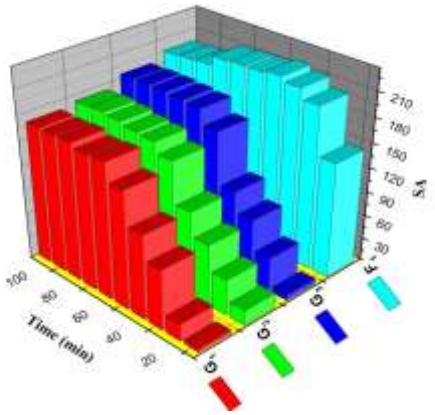

5A

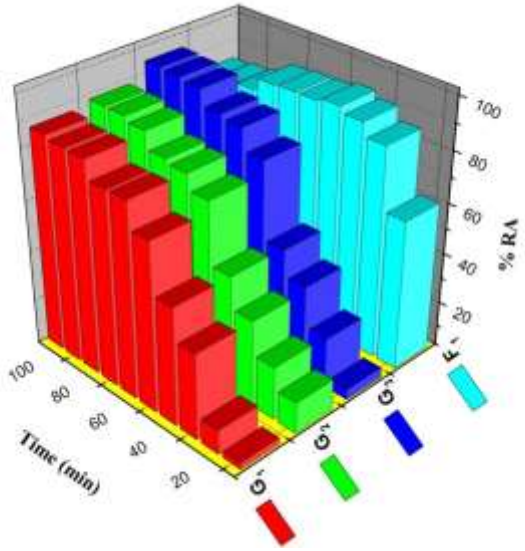

5B

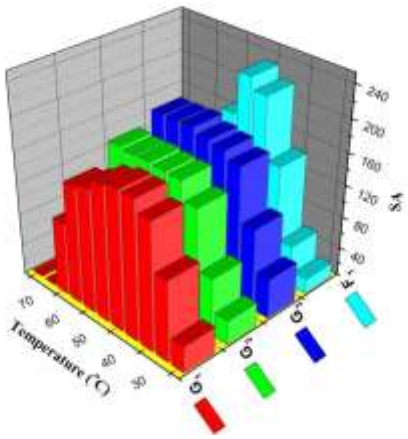

5C

ISSN 2278-2540 | DOI: 10.51583/IJLTEMAS | Volume XV, Issue VIII, August 2026

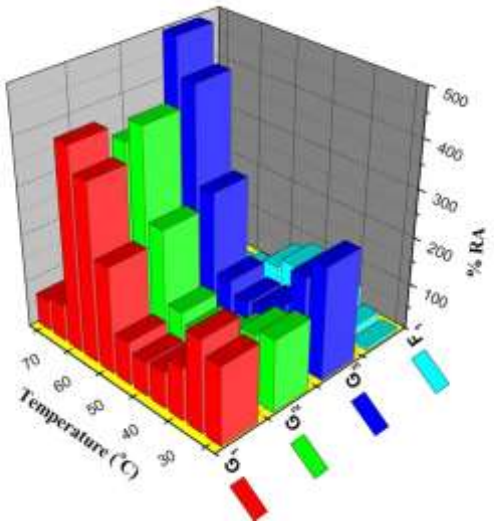

5D

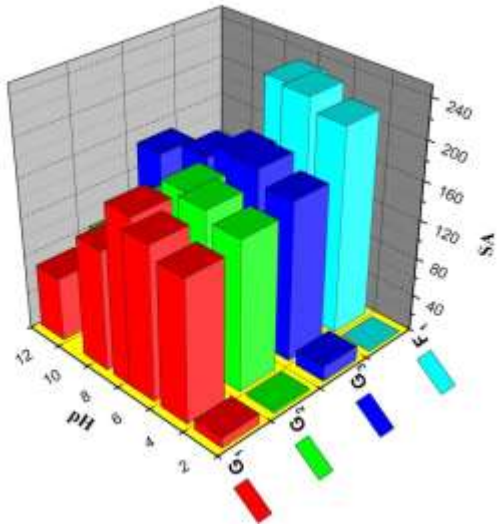

5E

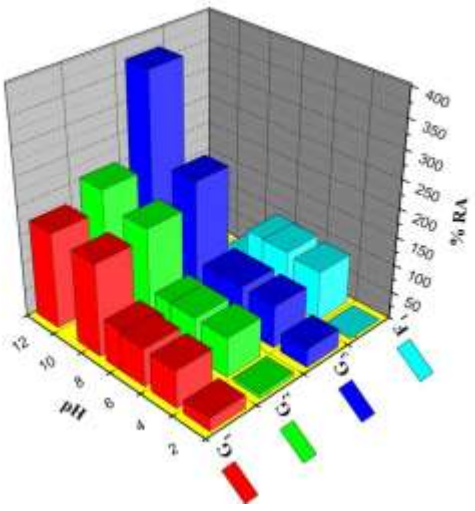

ISSN 2278-2540 | DOI: 10.51583/IJLTEMAS | Volume XV, Issue VIII, August 2026

5F

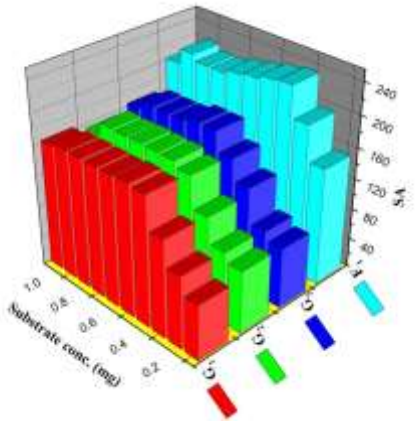

5G

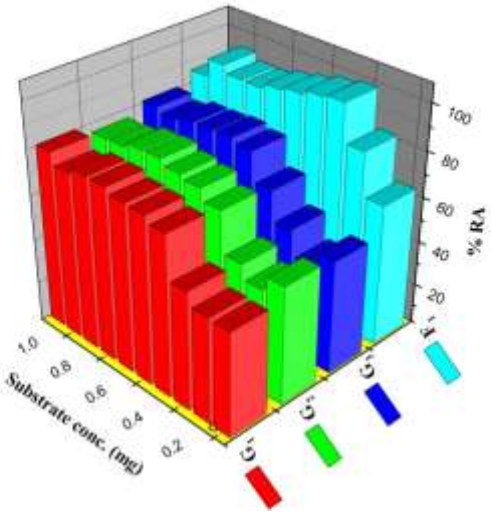

5H

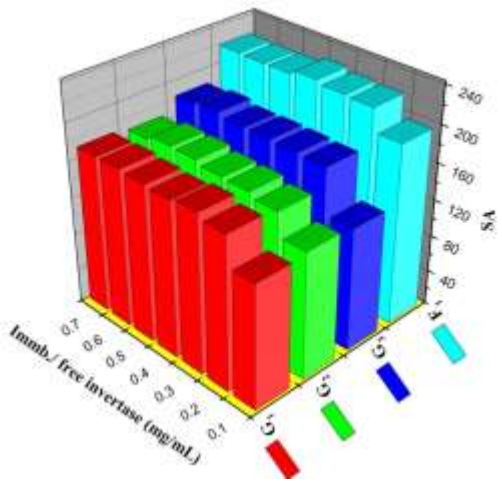

5I

ISSN 2278-2540 | DOI: 10.51583/IJLTEMAS | Volume XV, Issue VIII, August 2026

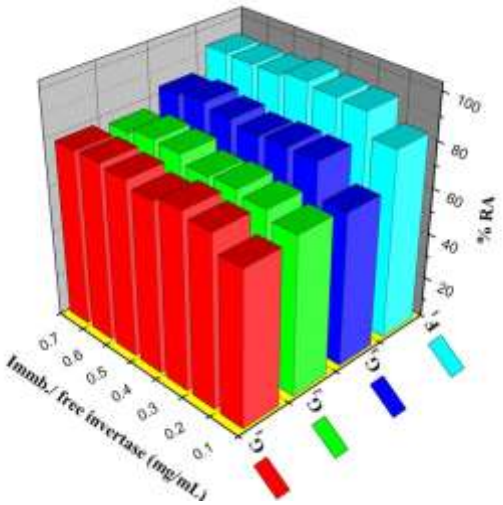

5J

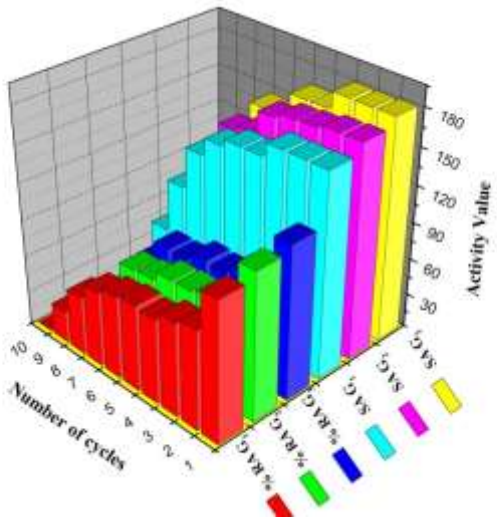

5K

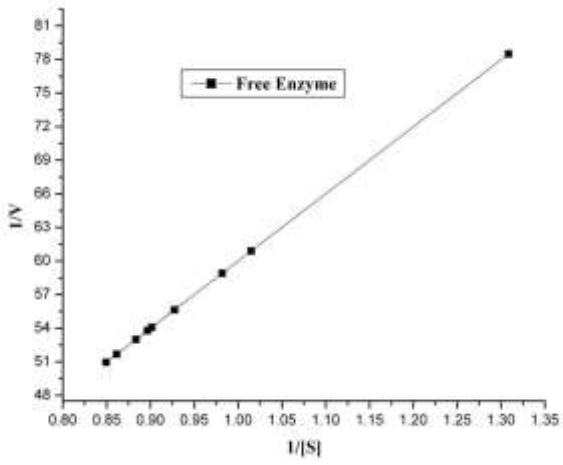

6A

ISSN 2278-2540 | DOI: 10.51583/IJLTEMAS | Volume XV, Issue VIII, August 2026

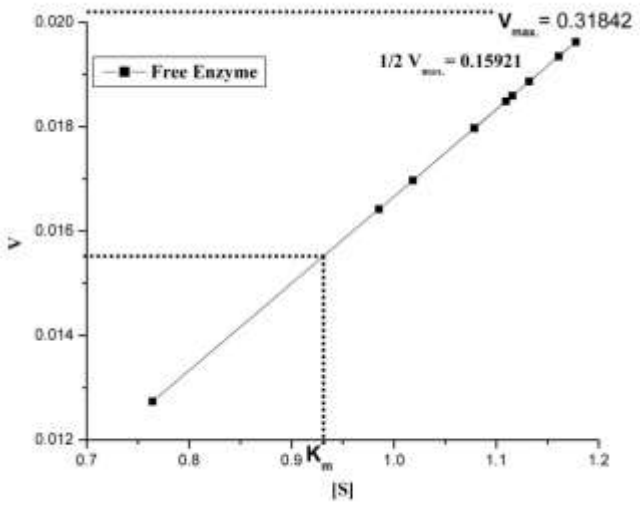

6B

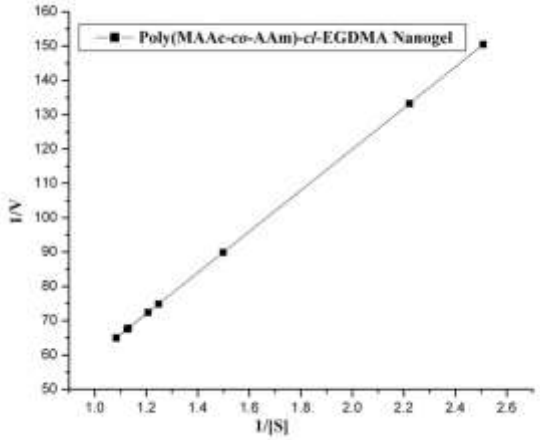

6C

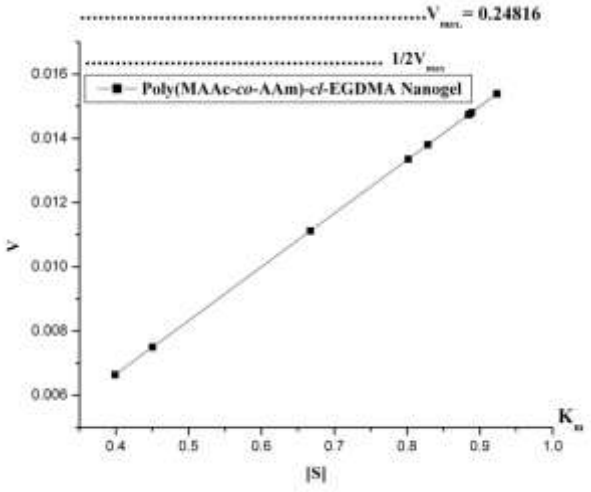

6D

ISSN 2278-2540 | DOI: 10.51583/IJLTEMAS | Volume XV, Issue VIII, August 2026

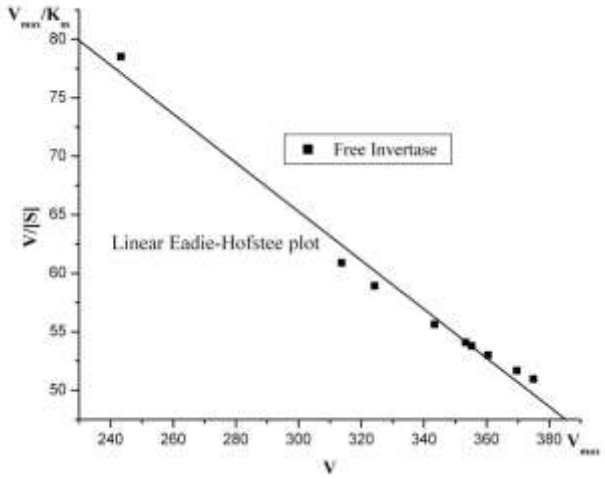

6E

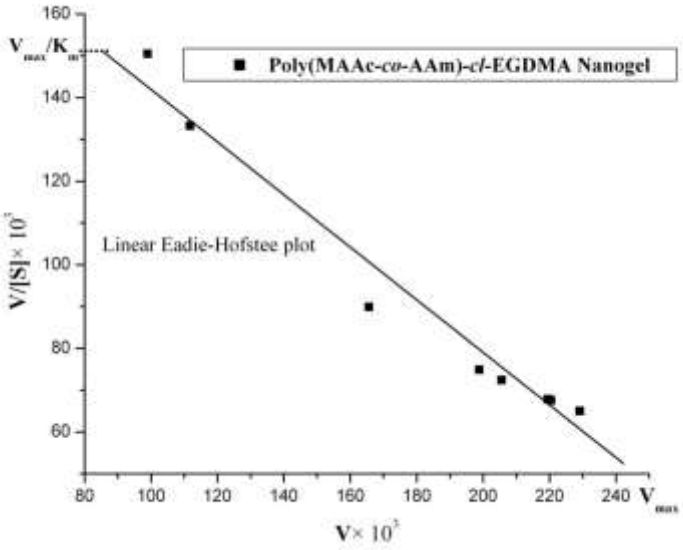

6F

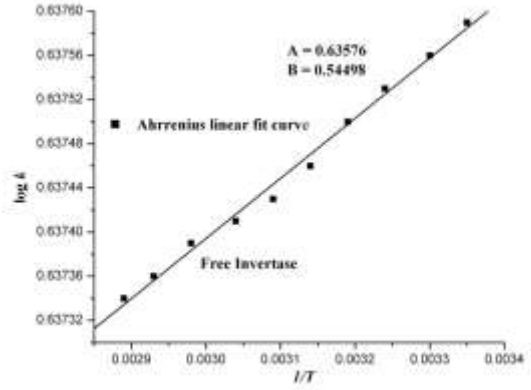

7A

ISSN 2278-2540 | DOI: 10.51583/IJLTEMAS | Volume XV, Issue VIII, August 2026

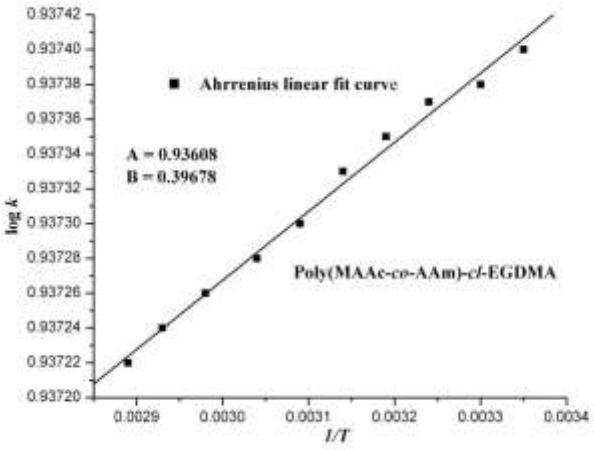

7B